

Di-trinucleon cluster resonances in $A = 6$ isobar nuclei

T. Yamagata,^{1,*} H. Akimune,¹ S. Nakayama,² M. Fujiwara,^{3,4} K. Fushimi,² M. B. Greenfield,⁵ K. Hara,³ K. Y. Hara,¹ H. Hashimoto,³ K. Ichihara,² K. Kawase,³ M. Kinoshita,¹ Y. Matsui,² K. Nakanishi,³ M. Ohta,¹ A. Shiokawa,¹ M. Tanaka,⁶ H. Utsunomiya,¹ and M. Yosoi⁷

¹*Department of Physics, Konan University, Kobe 658-8501, Japan*

²*Department of Physics, University of Tokushima, Tokushima 770-8502, Japan*

³*Research Center for Nuclear Physics, Osaka University, Osaka 567-0047, Japan*

⁴*Advance Photon Research Center, JAERI, Kizu 619-0215, Japan*

⁵*Department of Physics, International Christian University, Tokyo 113-0033, Japan*

⁶*Kobe Tokiwa College, Kobe 654-0838, Japan*

⁷*Department of Physics, Kyoto University, Kyoto 606-8502, Japan*

(Received 28 January 2005; published 24 June 2005)

The di-trinucleon clustering resonances of ${}^3\text{He} + {}^3\text{He}$ in ${}^6\text{Be}$ and $t + t$ in ${}^6\text{He}$ were studied via the ${}^6\text{Li}({}^3\text{He}, t\text{ }^3\text{He})$ and ${}^6\text{Li}({}^7\text{Li}, {}^7\text{Be}t)$ reactions at incident energies of 450 and 455 MeV, respectively. A new resonance in ${}^6\text{Be}$ was found at $E_x = 18.0 \pm 1.2$ MeV with a width of 9.2 ± 1.0 MeV in the binary decay channel of ${}^6\text{Be} \rightarrow {}^3\text{He} + {}^3\text{He}$. The resonance in ${}^6\text{He}$ previously reported was also observed at $E_x = 18.0 \pm 1.0$ MeV with a width of 9.5 ± 1.0 MeV in the binary decay channel of ${}^6\text{He} \rightarrow t + t$. The branching ratios of the resonances for each binary decay were both 0.7 ± 1.0 , which was larger than the branching ratio calculated in a statistical model by two orders of magnitude. The angular correlations measured for t and ${}^3\text{He}$ particles in the binary decay show a contribution dominantly from the multipolarity of $L = 1$. We suggest that the resonances are the members of the isobaric triplet of the 3P resonances in $A = 6$ nuclei.

DOI: 10.1103/PhysRevC.71.064316

PACS number(s): 27.20.+n, 24.30.Gd, 25.55.Kr, 25.70.Kk

I. INTRODUCTION

α clustering in nuclei is well known from light to heavy nuclei [1,2]. Cluster phenomena resulting from strong correlations among nucleons are general. For example, nuclear clusters other than the α cluster are observed and play an important role in nuclear structure and nuclear reactions [3,4]. Study of di-trinucleon clusters in the $A = 6$ triad— ${}^6\text{He}$, ${}^6\text{Li}$, ${}^3\text{H}$, and ${}^6\text{Be}$ —is an interesting subject. The trinucleon clusters and ${}^3\text{He}$ have quantum numbers $s = t = 1/2$ and $t_z = \pm 1/2$, which are the same as those of a neutron and a proton, respectively. In the $A = 6$ system, the di-trinucleon clusters are expected to exhibit multiplet spectra analogous to those expected in the two-nucleon system. The ground state of ${}^6\text{Li}$ is known to have a large component of a deuteronlike configuration, 3S_1 , in the LS -coupling model for the $t + {}^3\text{He}$ structure [5]. Here, the notation denotes $2S+1L_J$. In the two-nucleon system, however, the bound state is only the 3S with a small admixture of 3D state, and no 1S resonance exists. However, there may exist not only many bound states but also resonant states in the di-trinucleon system [6]. Therefore, we have a chance from investigation of the di-trinucleon system to study typical multiplet states in the two-fermion system. However, the existence of di-trinucleon clustering states is still a long-standing controversy.

In the LS -coupling scheme for the di-trinucleon system, Thompson and Tang predicted the multiplet spectra from the resonating group method (RGM) calculation [6]. They

predicted the 1P ($T = 0$) and 3P ($T = 1$) resonances at $E_x \sim 22$ MeV and the 1F ($T = 0$) and 3F ($T = 1$) resonances at $E_x \sim 29$ MeV in ${}^6\text{Li}$, which is higher than the P resonances by about 7 MeV [6]. Ohkura *et al.* performed a more elaborate calculation using the complex-scaled RGM (CSRGM) [7]. They predicted the 1P and 3P resonances in ${}^6\text{Li}$ around $E_x = 17$ MeV, and 1F and 3F resonances around 26 MeV. The excitation energies predicted for the P and F resonances are lower by about 3–5 MeV than those predicted by Thompson and Tang [6]. In the case of ${}^6\text{He}$ and ${}^6\text{Be}$, Thompson and Tang predicted the 3P and 3F resonances at $E_x \sim 19$ and ~ 26 MeV, respectively [6]. These values agreed well with those for the 3P and 3F resonances in ${}^6\text{Li}$ if the Coulomb displacement energy of 3.56 MeV is taken into account for the comparison of the energy spectra in the $A = 6$ system.

Experimentally, trinucleon cluster resonances in ${}^6\text{Li}$ and ${}^6\text{Be}$ were reported on the basis of radiative capture reactions [8–10] and of the phase shift analysis on the elastic scattering of polarized ${}^3\text{He}$ on ${}^3\text{H}$ and ${}^3\text{He}$ [11,12]. In the case of ${}^6\text{Li}$, Ventura *et al.* found evidence for the 3P_2 and 3F resonances at $E_x = 18.3$ and 26 MeV, respectively, from the ${}^3\text{He}(t,\gamma)$ reaction [9]. However, the results reported by Vlastou *et al.* from the elastic scattering of ${}^3\text{He}$ on ${}^3\text{H}$ [11] were not in agreement with those of Ventura *et al.* that the ${}^3P_{0,2}$ resonances exist at $E_x \sim 21$ MeV and the ${}^3F_{3,4}$ resonances at ~ 26 MeV. Vlastou *et al.* carefully investigated the resonances at $E_x \sim 20$ MeV and confirmed the 3P_2 resonance that was not observed by Ventura *et al.* in this excitation energy region [9]. The data reported from these studies are inconsistent with each other.

*Electronic address: yamagata@center.konan-u.ac.jp

In ${}^6\text{Be}$, experimental information is available only for the 3F resonances from the radiative capture reaction of ${}^3\text{He}$ on ${}^3\text{He}$ [10] and from the phase shift analysis of elastic scattering of polarized ${}^3\text{He}$ on ${}^3\text{He}$ [12]. However, these results were also not in agreement with each other. Thus, the issue of trinucleon clustering in $A = 6$ nuclei is currently inconclusive both theoretically and experimentally.

To settle the issue of trinucleon clustering in $A = 6$ nuclei, we pursued a different approach [13,14] than in the previous work: If the trinucleon clustering resonances are located above the trinucleon threshold energies, the resonances dominantly decay into binary trinucleon clusters. A coincidence measurement to detect the binary decay could be a powerful tool to probe trinucleon clustering resonances. Motivated by this expectation, we investigated the $t + t$ structure in ${}^6\text{He}$ and the $t + {}^3\text{He}$ structure in ${}^6\text{Li}$ via coincidence measurement by observing trinucleon-cluster decay in the ${}^6\text{Li}({}^7\text{Li}, {}^7\text{Be})$ reaction at 455 MeV and at $\theta_L = 0^\circ$ and the ${}^7\text{Li}({}^3\text{He}, \alpha)$ reaction at 450 MeV and at $\theta_L = 0^\circ$, respectively. These results have been published in Refs. [13,14].

Here, we summarize the results: We found a resonance at $E_x = 18.0 \pm 0.5$ MeV with a width of 7.7 ± 1.0 MeV in ${}^6\text{He}$ and a resonance at $E_x = 21$ MeV with a large width of 12 MeV in ${}^6\text{Li}$. As expected from our speculation, the resonances showed the binary triton and/or ${}^3\text{He}$ decay with a branching ratio of 80–90%, which were two orders of magnitude larger than the branching ratios estimated by a statistical-model calculation [13]. Based on the angular correlation of decay t and ${}^3\text{He}$ particles from ${}^6\text{Li}$, we assigned the angular momentum for the resonance in ${}^6\text{Li}$ to $L = 1$. Though the spin of the resonance in ${}^6\text{He}$ was not assigned in the experiment, the resonance energy was in good agreement with that for the 3P resonance calculated by Thomson and Tang [6]. Thus, we tentatively assigned the resonance in ${}^6\text{He}$ to 3P . Furthermore, the observed width of the resonance in ${}^6\text{Li}$ was found to be 12 MeV, much larger than the resonance width of 7.7 MeV in ${}^6\text{He}$ [13]. We concluded that the resonance in ${}^6\text{Li}$ consists of the P doublet, namely, the 1P ($T = 0$) state at $E_x = 18.0 \pm 0.5$ MeV and 3P ($T = 1$) state at $E_x = 22 \pm 1$ MeV [14].

In the present work we studied the trinucleon cluster structures as an extended study of the previous work [13,14], focusing our attention on the P resonances in ${}^6\text{He}$ and ${}^6\text{Be}$ via coincidence experiments measuring the branching ratios and angular correlation of the trinucleon decay. Since the previous assignment of the 21-MeV resonance in ${}^6\text{Li}$ to the 1P and 3P doublet [14] was made on the basis of the assumption that the 18.0-MeV resonance in ${}^6\text{He}$ is the 3P resonance [13], it was necessary to confirm that the angular momentum of this resonance in ${}^6\text{He}$ is $L = 1$, and thus we remeasured the ${}^6\text{Li}({}^7\text{Li}, {}^7\text{Be})$ reaction to do so. Although no experimental information on the 3P resonance in ${}^6\text{Be}$ has been reported, the 3P resonance should also exist at $E_x \sim 18$ MeV as isobaric analog resonances of ${}^6\text{He}$ and ${}^6\text{Li}$ according to the previous results [13,14]. Since the ${}^6\text{Li}({}^3\text{He}, t)$ reaction at $\theta_L = 0^\circ$ favors excitation of low-spin resonances, it would be an advantage to use this reaction to observe the 3P resonance in ${}^6\text{Be}$. We discuss the present results for ${}^6\text{He}$ and ${}^6\text{Be}$ in comparison with the previous results on ${}^6\text{Li}$ [14].

II. EXPERIMENT

The experiment was carried out by using the 455-MeV ${}^7\text{Li}$ and 450-MeV ${}^3\text{He}$ beams from the ring cyclotron at the Research Center for Nuclear Physics (RCNP), Osaka University. The target used was a self-supporting metallic foil of enriched ${}^6\text{Li}$ (95.4%) with a thickness of 0.6 mg/cm 2 . The target was tilted by 45° with respect to the beam direction to minimize the energy loss of the decay particles in the target. Reaction particles were analyzed by using the magnetic spectrograph “Grand Raiden” located at $\theta_L = 0^\circ$ and were detected with a focal plane detector system consisting of two multiwire drift chambers backed by a $\Delta E - E$ plastic scintillator telescope [15]. The aperture of the entrance slits of the spectrograph was ± 20 mrad horizontally and ± 30 mrad vertically. After passing through the target, the beams were stopped with a Faraday cup located inside the spectrograph. In each reaction, only the events within a ± 20 mrad vertical bin were sorted in an event-by-event mode by a software gate in a ray-trace method to define the recoil direction of the residual nuclei. Typical values of energy resolution were 800 keV and 340 keV for the $({}^7\text{Li}, {}^7\text{Be})$ and $({}^3\text{He}, t)$ reactions, respectively. The energy resolution for the $({}^3\text{He}, t)$ reaction was mainly limited by the energy spread of the incident beam, whereas that for the $({}^7\text{Li}, {}^7\text{Be})$ reaction was mainly limited by both the energy spread of the incident beam and the ${}^7\text{Be}$ -particle excitation ($E_x = 0.43$ MeV). Since the momentum acceptance of the spectrograph is 5%, the reaction spectra for excitation-energy regions from 3 to 43 MeV and from 0 to 33 MeV were measured in coincidence experiments for ${}^6\text{He}$ and ${}^6\text{Be}$, respectively.

Charged particles emitted from the resonances in ${}^6\text{He}$ and ${}^6\text{Be}$ excited via the $({}^7\text{Li}, {}^7\text{Be})$ and $({}^3\text{He}, t)$ reactions, respectively, were detected by using eight Si detectors (SSDs) with a thickness of 500 μm . In the previous measurement of the ${}^6\text{Li}({}^7\text{Li}, {}^7\text{Be})$ reaction, since we measured decay particles in various combinations of polar angles θ and azimuthal angles ϕ , the recoil direction of the outgoing ${}^6\text{He}$ was not well defined. As a result, the angular correlation was smooth over a wide angular range and thus the observed pattern was flat [13]. In the present measurement decay particles were detected in a single reaction plane at the azimuthal angle of $\phi = 0^\circ$. The SSDs were positioned at the angles between $\theta_L = 90^\circ$ and $\theta_L = 160^\circ$ at intervals of 10° and all at a distance of 25 cm from the target. A schematic view of the experimental setup is shown in Fig. 1.

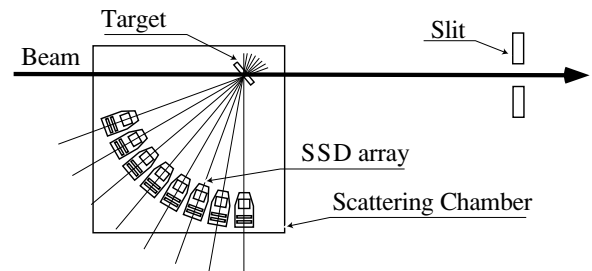


FIG. 1. A schematic view of the experimental setup.

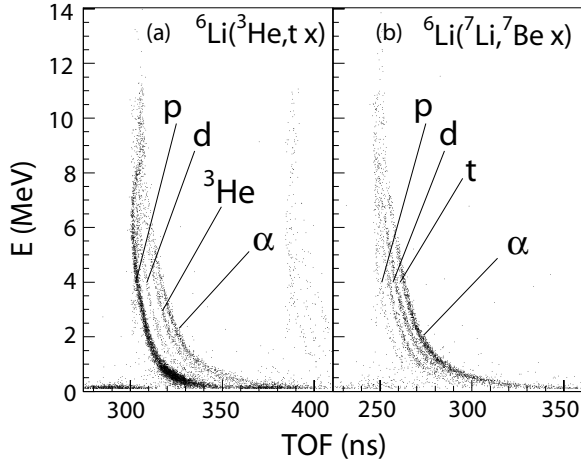


FIG. 2. Two-dimensional scatter plots of the coincidence events for identification of decay particles for (a) the (${}^3\text{He}, t$ x) and (b) (${}^7\text{Li}, {}^7\text{Be}$ x) reactions. The SSD used in this measurement is located at $\theta_L = 110^\circ$.

Because the threshold energies for the trinucleon-cluster decay are high (i.e., $E_x = 12.3$ MeV in ${}^6\text{He}$ and $E_x = 11.5$ MeV in ${}^6\text{Be}$) the energies of decay particles are low. A time-of-flight (TOF) technique was utilized for identification of decay particles. Each Si detector was backed by a $300\text{-}\mu\text{m}$ Si detector which was operated as an E detector or a veto detector for rejection of high-energy protons and deuterons that penetrated the $500\text{-}\mu\text{m}$ Si detectors.

Figure 2 shows the typical two-dimensional scatter plots for the (${}^3\text{He}, t$ x) and (${}^7\text{Li}, {}^7\text{Be}$ x) reactions. The events for t or ${}^3\text{He}$ particles were well separated from those for p , d , and α particles. Since the threshold energy attributed to the noise discrimination level of the detectors was set as low as possible (e.g., about 0.1 MeV), the missing number of low-energy particles resulting from the detector discrimination level remained small, at most 3%. A small contribution from ${}^{12}\text{C}$ contamination was recognized in the singles spectra measured with the ${}^6\text{Li}$ target. The ${}^{12}\text{C}$ contribution was checked by measuring the spectra with a ${}^{12}\text{C}$ target and was confirmed to be negligibly small in the coincidence spectra.

III. RESULTS AND ANALYSIS

A. The ${}^6\text{Li}({}^7\text{Li}, {}^7\text{Be } t)$ reaction

Figure 3 shows spectra for the ${}^6\text{Li}({}^7\text{Li}, {}^7\text{Be } t)$ reaction. The spectra observed in the present study are similar to those observed in the previous work [13]. The resonances observed in the singles spectra [Fig. 3(a)] at $E_x \sim 5, 15,$ and 25 MeV have been assigned to the soft-dipole resonance [16], the analog state of the dipole resonance at $E_x = 18$ MeV in ${}^6\text{Li}$ [17] and the analog of the α -cluster excitation in ${}^6\text{Li}$ [17,18], respectively. In the scatter plot of coincidence events for the ${}^6\text{Li}({}^7\text{Li}, {}^7\text{Be } t)$ reaction, as shown in Fig. 3(b), a locus along the kinematical threshold for $t + t$ decay is clearly identified. Similar loci were observed in every detector. Figure 3(c) shows a spectrum gated on the locus for the $t + t$ binary decay. A resonance was observed at $E_x = 18.0 \pm 1.0$ with a full width at half maximum

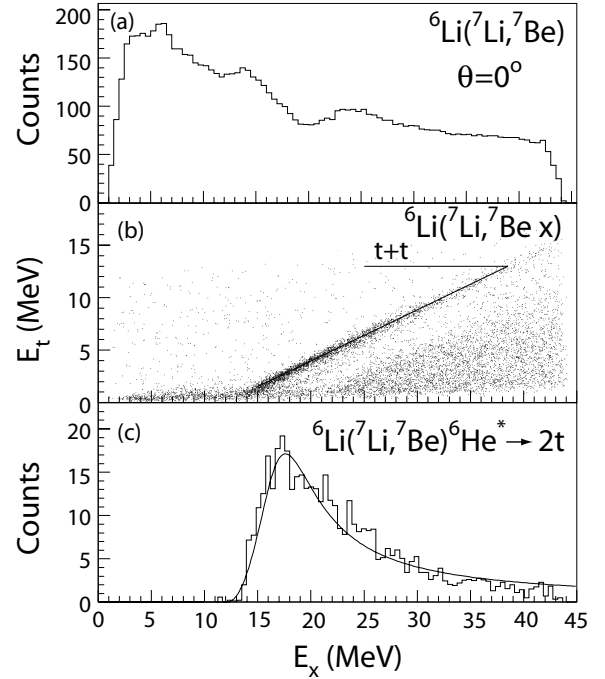


FIG. 3. (a) A singles spectrum for the ${}^6\text{Li}({}^7\text{Li}, {}^7\text{Be})$ reaction measured at $\theta_L = 0^\circ$ and at incident energy of 455 MeV. (b) A two-dimensional scatter plot of coincidence events for the ${}^6\text{Li}({}^7\text{Li}, {}^7\text{Be } t)$ reaction at $\theta_L = 110^\circ$. (c) A spectrum gated on the $t + t$ decay in the ${}^6\text{Li}({}^7\text{Li}, {}^7\text{Be})$ reaction. Accidental coincidence events have been subtracted. A solid curve shows the best fit to the data using the Breit-Wigner formula.

(FWHM) of 9.5 ± 1.0 MeV. These values are in agreement with those obtained in the previous work by Akimune *et al.* [13].

B. The ${}^6\text{Li}({}^3\text{He}, t {}^3\text{He})$ reaction

Figure 4 shows the spectra for the ${}^6\text{Li}({}^3\text{He}, t {}^3\text{He})$ reaction. The singles spectrum observed for the ${}^6\text{Li}({}^3\text{He}, t)$ reaction is similar to that obtained for the ${}^6\text{Li}({}^7\text{Li}, {}^7\text{Be})$ reaction. The resonances observed in the singles spectra [Fig. 4(a)] at $E_x \sim 15$ and 25 MeV have been assigned to the analog state of the dipole resonance at 18 MeV in ${}^6\text{Li}$ and the analog of the α -cluster excitation in ${}^6\text{Li}$ [17], respectively. The results for the singles ${}^6\text{Li}({}^3\text{He}, t)$ measurement has been published in Ref. [17]. In a scatter plot of coincidence events for the ${}^6\text{Li}({}^3\text{He}, t {}^3\text{He})$ reaction, as shown in Fig. 4(b), a locus along the kinematical threshold for ${}^3\text{He} + {}^3\text{He}$ decay is clearly identified. Similar loci were observed in every Si detector. Figure 4(c) shows a spectrum gated on the locus for the ${}^3\text{He} + {}^3\text{He}$ binary decay. The resonance was observed at $E_x = 18.0 \pm 1.2$ with a FWHM of 9.2 ± 1.3 MeV. These values are in excellent accordance with those obtained for the resonance in the ${}^6\text{Li}({}^7\text{Li}, {}^7\text{Be } t)$ reaction. This suggests that the resonances observed in ${}^6\text{He}$ and ${}^6\text{Be}$ at $E_x = 18$ MeV are isobaric analogs of each other. It is noted that the resonances observed in the binary decay channels in ${}^6\text{He}$ and ${}^6\text{Be}$ are not discernible in the singles spectra, but their existence is made clear via coincidence measurements.

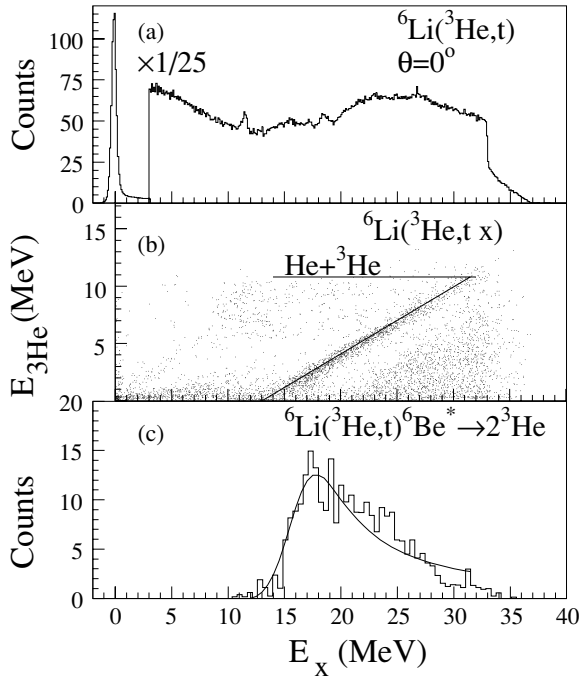


FIG. 4. (a) A singles spectrum for the ${}^6\text{Li}({}^3\text{He},t)$ reaction measured at $\theta_L = 0^\circ$ and at incident energy of 450 MeV. (b) A two-dimensional scatter plot of coincidence events for the ${}^6\text{Li}({}^3\text{He},t,{}^3\text{He})$ reaction at $\theta_L = 110^\circ$. (c) A spectrum gated on the ${}^3\text{He} + {}^3\text{He}$ decay in the ${}^6\text{Li}({}^3\text{He},t)$ reaction. Accidental coincidence events have been subtracted. A solid curve shows the best fit to the data using the Breit-Wigner formula.

C. The angular correlation of the t and ${}^3\text{He}$ decay

Since we measure the reaction particles at $\theta_L = 0^\circ$, the spin alignment of the residual nuclei is expected. Angular correlation of decay particles provides a unique spin assignment for the initial states. We investigated the angular correlation of the decay tritons and ${}^3\text{He}$ from the resonances observed at $E_x = 18$ MeV in both ${}^6\text{He}$ and ${}^6\text{Be}$. Figure 5(a) shows the angular correlation pattern for ${}^6\text{He}$ in the excitation energy region of $12.3 \leq E_x \leq 43$ MeV, in which most of the resonance yield is included. The observed correlation patterns were fitted by a Legendre polynomial with orders up to $L = 3$, $W(\theta_{\text{c.m.}}) = N(1 + \alpha_1 P_1^2 + \alpha_2 P_2^2 + \alpha_3 P_3^2)$, where N , α_L s, and $P_L(\theta_{\text{c.m.}})$ are a normalization factor, the expansion coefficients, and the Legendre function with order L , respectively; $\theta_{\text{c.m.}}$ is measured in the rest frame of ${}^6\text{He}$ and ${}^6\text{Be}$ by taking into account the recoil effect. The fitted values for N and α_L s are listed in Table I. Since $\alpha_1 \gg \alpha_{2,3}$, the angular momentum for the resonance at $E_x = 12.3 \sim 43$ MeV in ${}^6\text{He}$ is suggested to be $L = 1$. However, it is necessary to increase the value of α_3 to fit the $W(\theta_{\text{c.m.}})$ in the excitation energy region of $20 \leq E_x \leq 35$ MeV in ${}^6\text{He}$, as shown Fig. 5(b) and Table I. This suggests the existence of an $L = 3$ component in this excitation energy region.

Figure 5(c) shows the angular correlation of the decay ${}^3\text{He}$ from the 18-MeV resonance in ${}^6\text{Be}$. The data were fitted with a truncated series of Legendre polynomials. The fitted values for N and α_L s obtained in the $({}^3\text{He},t,{}^3\text{He})$ reaction are listed in

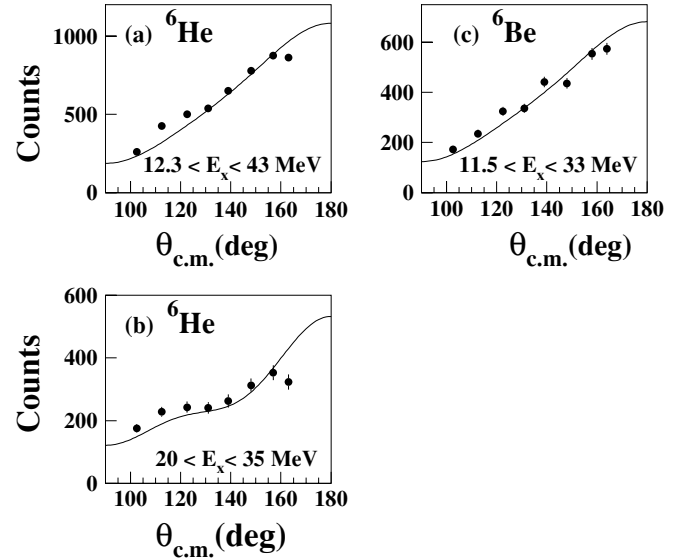


FIG. 5. Angular correlation patterns of t in the ${}^6\text{Li}({}^7\text{Li},{}^7\text{Be})t$ reaction in the excitation energy regions of (a) $12.3 \leq E_x \leq 43$ MeV and (b) $20 \leq E_x \leq 35$ MeV and of (c) ${}^3\text{He}$ in the ${}^6\text{Li}({}^3\text{He},t,{}^3\text{He})$ reaction in the excitation energy region of $11.5 \leq E_x \leq 33$ MeV. The solid curves show the results of fitting with the Legendre polynomial.

Table I. Again, the large value for α_1 suggests $L = 1$ for the angular momentum of the resonance. In the case of ${}^6\text{Be}$, an apparent effect of an $L = 3$ resonance was not found. This may be because this reaction favors low-spin excitation.

D. Analysis with the Breit-Wigner one-level formula

To extract the resonance parameters, the spectral shapes of the resonances in ${}^6\text{He}$ and ${}^6\text{Be}$ shown in Figs. 3(c) and 4(c), respectively, were fitted by using the Breit-Wigner one-level formula [19] in accordance with the same prescription used in the previous work [13]. We assumed the triple differential cross section $d^3\sigma(E_x)/d\Omega d\Omega_3 dE_x$ to be

$$\frac{d^3\sigma(E_x)}{d\Omega d\Omega_3 dE_x} \propto \frac{\Gamma_3}{(E_x - E_R)^2 + (\Gamma/2)^2}, \quad (1)$$

where Ω_3 , E_R , Γ , and Γ_3 are the solid angle for t (${}^3\text{He}$), the resonance energy, the total width, and the partial width for

TABLE I. N and α_L s obtained in the fitting of the angular correlation.

	N	α_1	α_2	α_3
${}^6\text{He}$ $12.3 \leq E_x \leq 43$ MeV	185 ± 5	4.2 ± 0.2	0.1 ± 0.1	0.6 ± 0.2
${}^6\text{He}$ $20 \leq E_x \leq 35$ MeV	121 ± 5	1.8 ± 0.1	0.0 ± 0.1	1.6 ± 0.1
${}^6\text{Be}$ $11.5 \leq E_x \leq 33$ MeV	124 ± 5	3.9 ± 0.2	0.1 ± 0.1	0.6 ± 0.2

TABLE II. Resonance parameters for the trinucleon states in $A = 6$ nuclei.

	${}^6\text{He}^a$	${}^6\text{He}^b$	${}^6\text{Li}^c$	${}^6\text{Be}^b$	$2S+1L$
E_R (MeV) ^d			18.0 ± 0.5		1P
FWHM (MeV)			5.0 ± 0.5		
θ^{2d}			1.0 ± 0.4		
Γ' (MeV) ^d			3 ± 1		
E_R (MeV) ^d	18.0 ± 0.5	18.0 ± 1.0	22.0 ± 1.0	18.0 ± 1.2	3P
FWHM (MeV)	7.7 ± 1.0	9.5 ± 1.0	8 ± 1	9.2 ± 1.3	
θ^{2d}	1.0 ± 0.4	1.0 ± 0.2	1.0 ± 0.4	1.0 ± 0.2	
Γ' (MeV) ^d	3 ± 1	3 ± 1	3 ± 1	3.5 ± 1	

^aTaken from Ref. [13].^bPresent work.^cTaken from Ref. [14].^dDerived from Eq. (1).

t (${}^3\text{He}$) decay, respectively. The width Γ_3 is expressed as [20]

$$\Gamma_3 = \frac{2\hbar}{R} \sqrt{\frac{2E}{\mu}} \theta^2 p_L, \quad (2)$$

where R , E , μ , θ^2 , and p_L are the interaction radius of ${}^6\text{He}$ (${}^6\text{Be}$), the decay energy of t (${}^3\text{He}$) in the center-of-mass system, a reduced mass for t (${}^3\text{He}$), a dimensionless reduced width ($\theta^2 \leq 1$), and penetrability with an angular momentum L , respectively. The interaction radius is given by $R = r_0(A_3^{1/3} + A_3^{1/3})$, where A_3 is the mass of t (${}^3\text{He}$), and $r_0 = 1.4$ fm was chosen [21]. Since the 18-MeV resonance in ${}^6\text{He}$ (${}^6\text{Be}$) is located well above the neutron (proton) threshold energy, 0.93 MeV (-1.37 MeV), the resonance is expected to mainly decay by triton (${}^3\text{He}$) and neutron (proton) emissions. We assumed that $\Gamma = \Gamma_3 + \Gamma'$, where Γ' is a partial width for neutron (proton) decay. The partial width Γ' was assumed to be constant for simplicity.

Figure 6 shows the calculated shapes for the resonance in ${}^6\text{He}$, where $E_R = 18.0$ MeV and $L = 1$ were assumed for the resonance, while the θ^2 and Γ' were allowed to vary as free parameters. The calculated resonance width decreases as θ^2 . To fit the observed resonance shape we should increase both θ^2 and Γ' . From this fitting procedure the values of E_R , θ^2 , and Γ' and their uncertainties were evaluated. The best values of these parameters obtained with this fitting procedure are listed in Table II, and the best fitted curves are shown in

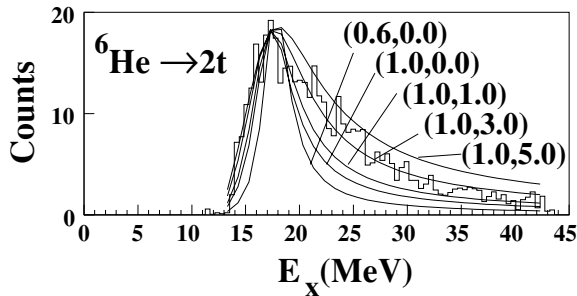


FIG. 6. Various resonance shapes in ${}^6\text{He}$ obtained by changing the parameters (θ^2 , Γ').

Figs. 3(c) and 4(c). The branching ratios for the trinucleon decay, Γ_3/Γ , averaged over the excitation energy up to 35 MeV were observed to be $70 \pm 10\%$ in the analysis of both ${}^6\text{He}$ and ${}^6\text{Be}$; these results are consistent with the previous measurements [13,14].

IV. DISCUSSION

A. Branching ratios calculated by the statistical model

The observed branching ratios for the binary decay from the resonances at $E_x = 18$ MeV in ${}^6\text{He}$ and ${}^6\text{Be}$ were compared with the results calculated in a simple statistical model [22]. Although there is a question whether or not the statistical-model calculation is applicable for light nuclei, an order-of-magnitude estimate should be valuable for the purpose of interpreting the experimental results.

Since the resonance is located well above the neutron (proton) threshold, only the neutron (proton) and trinucleon decays were taken into account as decay processes of the resonance. By assuming that the binary trinucleon decay and the neutron (proton) decay occur as fission and evaporation processes, the ratio of the widths can be expressed as [22]

$$\frac{\Gamma'}{\Gamma_3} = \frac{4A^{2/3}a_f(E_x - B_n)}{K_0a_n[2a_f^{1/2}(E_x - E_f)^{1/2} - 1]} \times \exp[2a_n^{1/2}(E_x - B_n)^{1/2} - 2a_f^{1/2}(E_x - E_f)^{1/2}], \quad (3)$$

where a_n , a_f , B_n , E_f , and K_0 are the level density parameters appropriate to the spherical shape and to the saddle shape, the neutron (proton) binding energy, the fission barrier for the binary trinucleon decay, and a constant parameter $K_0 = \hbar^2/2mr_0^2 \approx 10$ MeV, respectively. The fission barrier is $E_f = E_{\text{th}} + E_C$, where E_{th} and E_C are the threshold energy and the Coulomb potential for the binary trinucleon decay, respectively.

In the case of ${}^6\text{He}$, assuming $a_f \approx a_n = A/8$ in the Fermi gas model, and using $B_n = 0.97$ MeV, $E_{\text{th}} = 12.31$ MeV, and $E_C \sim 0.7$ MeV, gives a ratio of $\Gamma'/\Gamma_3 \sim 2 \times 10^2$ at $E_x = 18$ MeV. Since $\Gamma' > \Gamma_3$, the branching ratio for the binary t decay is expected to be $\Gamma_3/\Gamma \sim \Gamma_3/\Gamma' \sim 5 \times 10^{-3}$, which is smaller than the experimental value of 0.7 by about two orders

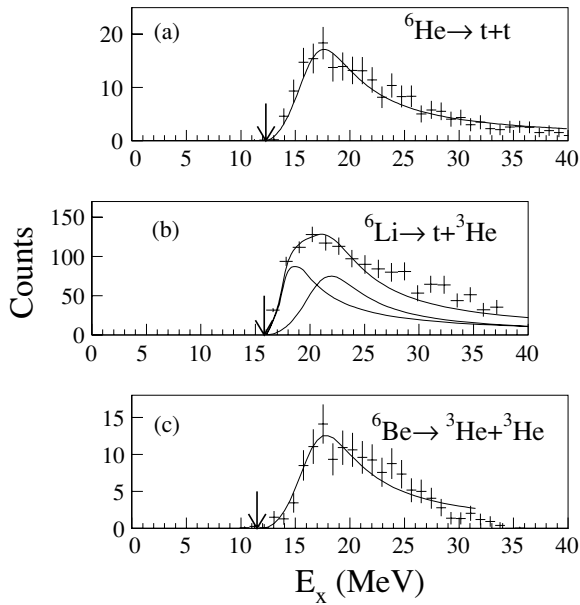


FIG. 7. Observed spectra for the P states in the $A = 6$ triad. The ${}^6\text{Li}$ spectrum is taken from Ref. [14]. The horizontal positions of the spectra are adjusted such that the isobaric analog states (0^+ , $T = 1$) in each nucleus might coincide. Arrows show threshold energies for the di-trinucleon decay.

of magnitude. In the case for ${}^6\text{Be}$, a similar calculation can be made using the proton binding energy $B_p = -1.37$ MeV, $E_{\text{th}} = 11.49$ MeV, and $E_C \sim 2.8$ MeV. The branching ratio calculated for the ${}^3\text{He} + {}^3\text{He}$ decay at $E_x = 18$ MeV is $\Gamma_3/\Gamma \sim \Gamma_3/\Gamma' \sim 1 \times 10^{-3}$, which is also smaller than the observed branching ratio by more than two orders of magnitude. The results for both ${}^6\text{He}$ and ${}^6\text{Be}$ suggest that the observed peaks at $E_x = 18$ MeV is not due to merely the threshold

effect and that decay of the 18-MeV resonances into t and ${}^3\text{He}$ is not statistical but due to the trinucleon clustering structures.

B. 3P ($T = 1$) and 1P ($T = 0$) resonances in the $A = 6$ triad

In Fig. 7, the resonance shapes observed in the trinucleon-binary decay channels in ${}^6\text{He}$ and ${}^6\text{Be}$ are shown together with that in ${}^6\text{Li}$ reported by Nakayama *et al.* [14]. Since the resonances in ${}^6\text{He}$ and ${}^6\text{Be}$ are observed at very similar excitation energies of $E_x \sim 18$ MeV and with similar widths of ~ 9 MeV, the resonances are concluded to be the isobaric analogs of each other. From the angular correlation of the binary decay, both the resonances are assigned to $L = 1$. Therefore, it is reasonable to assign them to be the 3P ($T = 1$) resonances.

In ${}^6\text{Li}$, a ~ 12 -MeV-wide resonance which is broader than the widths of the corresponding resonances in ${}^6\text{He}$ and ${}^6\text{Be}$, has been observed at $E_x \sim 21$ MeV. From the angular correlation measurement, the resonance has been assigned to 1P and/or 3P states. The 1P ($T = 0$) resonance should exist only in ${}^6\text{Li}$. Therefore, the broader width of the resonance in ${}^6\text{Li}$ may be due to overlapping of the 1P and 3P resonances. We decomposed the 21-MeV resonance in ${}^6\text{Li}$ into two resonances, one at $E_x = 22.0 \pm 1.0$ MeV with a width of 8 ± 1 MeV and the other at $E_x = 18 \pm 0.5$ MeV with a width of 5 ± 0.5 MeV. The former was assigned to be a 3P resonance and the latter a 1P [14], one, as shown in Fig 7(b). Upon subtracting the Coulomb displacement energy of 3.56 MeV in ${}^6\text{Li}$, good correspondence in the excitation energies and widths are found for the 3P resonances in three nuclei. Thus, for the first time, the complete set of 1P and 3P resonances in the $A = 6$ triad has been observed.

C. Comparison of the P resonances with other results

In Fig. 8, theoretical predictions for the trinucleon resonances as well as the previous and present experimental results

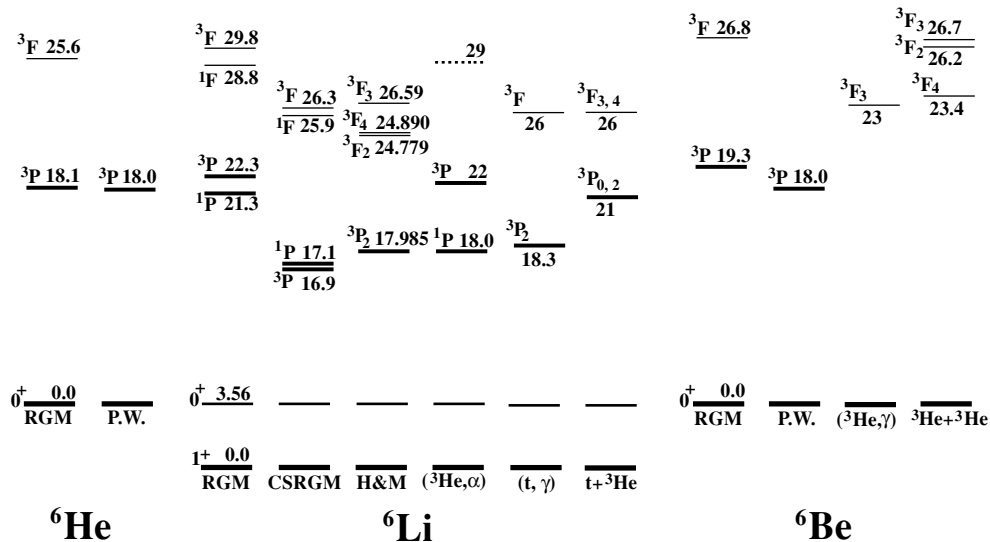


FIG. 8. The trinucleon clustering resonances in the $A = 6$ triad locate above the trinucleon decay threshold energies. RGM, CSRGM, and H&M denote the theoretical results in Refs. [6,7], and [23], respectively. $({}^3\text{He},\alpha)$, P.W., (t,γ) , $t + {}^3\text{He}$, $({}^3\text{He},\gamma)$, and ${}^3\text{He} + {}^3\text{He}$ denote the experimental results given in Ref. [14], in the present work, and in Refs. [9–12], respectively. The ground states and 3P resonances are shown with the thick lines.

are shown. The 3P resonance was reported only in ^6Li and no information is available for the 1P resonance.

Vlastou *et al.* reported the $^3P_{0,2}$ resonance at $E_x \sim 21$ MeV in ^6Li [11] from the phase shift analysis of the elastic scattering of ^3He on ^3H . This excitation energy is roughly equal to the present excitation energy of $E_x = 22$ MeV. However, Ventura *et al.* reported the 3P_2 resonance from the radiative capture reaction at $E_x = 18.3$ MeV [9], which is about 3 MeV lower than that reported by Vlastou and the present result. To consistently interpret the data on ^6Li from the radiative capture and the elastic scattering of the $t + ^3\text{He}$, Mondragón *et al.* reanalyzed both data sets simultaneously and showed that the 3P_2 resonance in ^6Li should exist at $E_x = 17.985 \pm 0.025$ MeV [23], which is consistent with the results obtained by Ventura *et al.* [9]. The result reported by Mondragón *et al.* was roughly reproduced with the CSRGM calculation [7], and it disagreed with the RGM calculation [6]. However, the excitation energies observed presently for the 3P resonances are consistent with the RGM prediction [6] and are inconsistent with the results in Ref. [23] and the CSRGM prediction [7].

The excitation energy observed presently for the 1P resonance in ^6Li is not consistent with the RGM and CSRGM calculations. The splitting energy observed in ^6Li between the 1P ($T = 0$) and 3P ($T = 1$) resonances is 4 MeV, whereas the RGM calculation predicts ~ 1 MeV. The splitting energies are 0.2–0.4 MeV in the CSRGM calculation, which are much smaller than the present result. The strength of the spin- or isospin-dependent interactions between two trinucleon

clusters may be larger than those involved in the theoretical calculations.

V. CONCLUDING REMARK

We investigated the di-trinucleon cluster resonances in isobaric triplet nuclei of ^6He , ^6Li , and ^6Be . We observed a complete set of 3P and 1P resonances for the first time. The observed excitation energies for these resonances did not agree with the CSRGM prediction, but they partly agreed with the RGM predictions. The treatment of the di-trinucleon system seems to be a simple two-body problem in the zeroth-order approximation. However, unlike the two-nucleon system the firm existence of the 3P resonances has been established in the di-trinucleon system. We hope that the complete spectra of the two-fermion system will be unveiled in the near future.

ACKNOWLEDGMENTS

The experiments were performed at the Research Center for Nuclear Physics, Osaka University, under Program Nos. E172, E184, and E190. The authors are grateful to the staff of the RCNP cyclotron for their support. This work was supported partly by the Grant-in-Aid (Nos. 13640304 and 16540257) by the Japan Ministry of Education, Culture, Sports, Science, and Technology and by the Japan Society for Promotion of Science (JSPS).

-
- [1] K. Ikeda, J. Phys. Soc. Jpn. Suppl. **58**, 277 (1989).
 - [2] H. Horiuchi, J. Phys. Soc. Jpn. Suppl. **58**, 7 (1989).
 - [3] H. J. Rose and G. A. Jones, Nature **309**, 245 (1984).
 - [4] M. Freer, *et al.*, Phys. Rev. Lett. **82**, 1383 (1999).
 - [5] Y. M. Shin, D. M. Skopik, and J. J. Murphy, Phys. Lett. **55B**, 297 (1975).
 - [6] D. R. Thompson and Y. C. Tang, Phys. Rev. Lett. **19**, 87 (1967); Nucl. Phys. **A106**, 591 (1968).
 - [7] H. Ohkura, T. Yamada, and K. Ikeda, Prog. Theor. Phys. **94**, 47 (1995).
 - [8] S. L. Blatt, A. M. Young, S. C. Ling, K. J. Moon, and C. D. Porterfield, Phys. Rev. **176**, 1147 (1968); A. M. Young, S. L. Blatt, and R. G. Seyler, Phys. Rev. Lett. **25**, 1764 (1970).
 - [9] E. Ventura, C. C. Chang, and W. E. Meyerhof, Nucl. Phys. **A173**, 1 (1971), and references therein.
 - [10] E. Ventura, J. Calarco, C. C. Chang, E. D. Diener, E. Kuhlmann, and E. Meyerhof, Nucl. Phys. **A219**, 157 (1974).
 - [11] R. Vlastou, J. B. A. England, O. Karban, and S. Baird, Nucl. Phys. **A292**, 29 (1977).
 - [12] R. Vlastou, J. B. A. England, O. Karban, S. Baird, and Y.-W. Lui, Nucl. Phys. **A303**, 368 (1978).
 - [13] H. Akimune, T. Yamagata, S. Nakayama, Y. Arimoto, M. Fujiwara, K. Fushimi, K. Hara, M. Ohta, A. Shiokawa, M. Tanaka, H. Utsunomiya, K. Y. Hara, H. P. Yoshida, and M. Yosoi, Phys. Rev. C **67**, 051302(R) (2003).
 - [14] S. Nakayama, T. Yamagata, H. Akimune, M. Fujiwara, K. Fushimi, M. B. Greenfield, K. Hara, K. Y. Hara, H. Hashimoto, K. Ichihara, K. Kawase, H. Matsui, K. Nakanishi, M. Sakama, M. Tanaka, and M. Yosoi, Phys. Rev. C **69**, 041304(R) (2004).
 - [15] M. Fujiwara, H. Akimune, I. Daito, H. Fujimura, Y. Fujita, K. Hatanaka, H. Ikegami, I. Katayama, K. Nagayama, N. Matsuoka, S. Morinobu, T. Noro, M. Yoshimura, H. Sakaguchi, Y. Sakemi, A. Tamii, and M. Yosoi, Nucl. Instrum. Methods Phys. Res. A **422**, 484 (1999).
 - [16] S. Nakayama, T. Yamagata, H. Akimune, I. Daito, H. Fujimura, Y. Fujita, M. Fujiwara, K. Fushimi, T. Inomata, H. Kohri, N. Koori, K. Takahisa, A. Tamii, M. Tanaka, and H. Toyokawa, Phys. Rev. Lett. **85**, 262 (2000).
 - [17] T. Yamagata, S. Nakayama, H. Akimune, M. Fujiwara, K. Fushimi, M. B. Greenfield, K. Hara, K. Y. Hara, H. Hashimoto, K. Ichihara, K. Kawase, M. Kinoshita, H. Matsui, K. Nakanishi, M. Tanaka, H. Utsunomiya, and M. Yosoi, Phys. Rev. C **69**, 044313 (2004).
 - [18] S. Nakayama, T. Yamagata, H. Akimune, I. Daito, H. Fujimura, Y. Fujita, M. Fujiwara, K. Fushimi, M. B. Greenfield, H. Kohri, N. Koori, K. Takahisa, A. Tamii, M. Tanaka, and H. Toyokawa, Phys. Rev. Lett. **87**, 122502 (2001).
 - [19] J. M. Blatt and V. F. Weisskopf, *Theoretical Nuclear Physics* (Wiley, New York, 1952), p. 391.
 - [20] C. E. Rolfs and W. S. Rodney, *Cauldrons in the Cosmos* (University of Chicago Press, Chicago, 1988), p. 178.
 - [21] J. B. Marion and F. C. Young, *Nuclear Reaction Analysis* (North-Holland, Amsterdam, 1968), p. 84.
 - [22] R. Vandenbosch and J. R. Huizenger, *Nuclear Fission* (Academic Press, New York, 1973), p. 233.
 - [23] E. Hernández and A. Mondragón, J. Phys. G **16**, 1339 (1990); A. Mondragón and E. Hernández, Phys. Rev. C. **41**, 1975 (1990).